frontiers in Materials

ORIGINAL RESEARCH
published: 10 September 2019
doi: 10.3389/fmats.2019.00219

Boosting Oxygen Reduction Performance of Manganese Oxide in Alkaline Media by Three-Dimensional Highly Ordered Conductive Porous Framework

Xiaofen Xiao[1,2], *Zhengsong Fang*[1] *and Dingshan Yu*[1]*

[1] *Key Laboratory for Polymeric Composite and Functional Materials of Ministry of Education, Key Laboratory of High Performance Polymer-Based Composites of Guangdong Province, School of Chemistry, Sun Yat-sen University, Guangzhou, China,* [2] *Collaborative Innovation Center for Intelligent New Energy Vehicle School of Automotive Studies, Tongji University, Shanghai, China*

MnO_2 has been widely used as an alternative candidate for oxygen reduction reaction owing to its abundance, low cost, and environmental compatibility. However, bulk MnO_2 as electrocatalysts is still suffering from serious active sites agglomeration and poor conductivity, resulting in low utilization of catalysts and sluggish reaction kinetics. In view of this, we fabricated a 3D highly ordered porous MnO_2@Ni-pc nanocomposite and significantly enhance ORR performance of MnO_2 with high onset potential of 1.04 V and half-wave potential of 0.89 V as well as a large limiting current density of 4.07 mA cm^{-2}, being even comparable to the commercial Pt/C. This nano-engineering technique is suitable for various catalysts that can be attached onto the 3D highly ordered porous framework, which provides new opportunities in designing electrode structures to boost the performance of bulk materials.

Keywords: manganese oxide, electrocatalyst, oxygen reduction reaction, nanocomposite, 3D ordered porous scaffold

OPEN ACCESS

Edited by:
Zhonghua Xiang,
Beijing University of Chemical Technology, China

Reviewed by:
Bao Yu Xia,
Huazhong University of Science and Technology, China
Liang Zhou,
Wuhan University of Technology, China

***Correspondence:**
Dingshan Yu
yudings@mail.sysu.edu.cn

Specialty section:
This article was submitted to Energy Materials, a section of the journal Frontiers in Materials

Received: *12 July 2019*
Accepted: *26 August 2019*
Published: *10 September 2019*

Citation:
Xiao X, Fang Z and Yu D (2019) Boosting Oxygen Reduction Performance of Manganese Oxide in Alkaline Media by Three-Dimensional Highly Ordered Conductive Porous Framework. Front. Mater. 6:219. doi: 10.3389/fmats.2019.00219

INTRODUCTION

Electrocatalysts for the oxygen reduction reaction (ORR) are of vital importance for many renewable energy applications such as metal-air batteries and fuel cells (Bashyam and Zelenay, 2006; Lefèvre et al., 2009; Wu et al., 2011). Noble Pt-based materials have shown the most efficient ORR performance but restricted severely by high cost, poor stability, and scarcity (Jaouen et al., 2011; Morozan et al., 2011b). Hence, a variety of catalysts based on non-precious metal oxides (Co_3O_4, FeO_x, and MnO_x etc.) have been widely investigated as alternative candidates for ORR owing to their abundance, low cost and environmental compatibility (Zhou et al., 2011). Nonetheless, bulk metal oxide catalysts as electrocatalysts are always suffering from some problems such as poor conductivity and serious agglomeration of active sites. Recently, many researches have demonstrated that there are various methods to effectively boost the performance of bulk metal oxide electrocatalysts through regulating their chemical components, conductivity, and microstructures. In addition, macrostructure, mechanical properties, and electrocatalyst/substrate contact of practical catalyst electrodes are also very important to achieve the maximum utilization

of electrocatalysts. Some materials such as graphene (Gong et al., 2013), Ni network (Chang et al., 2011), or carbonaceous nanofoam (Morozan et al., 2011a) have been widely used as conductive substrate to enhance the catalytic performance of electrocatalysts. However, most of reported nanocomposites can only satisfy one or several requirements of ideal electrocatalyst (**Figure 1a**). There are still big challenges to concurrently achieve highly ordered porous nanostructure and efficient electrons/ions pathways for electrocatalysts (Liu et al., 2011; Morozan et al., 2011a).

Due to the long-range periodicity of nanostructure, high volume fraction, and unique optical response behaviors, photonic crystal structures offer a way out for solving difficulties above-mentioned. The unique 3D ordered porous frameworks have been adopted for a myriad of applications from thin-film electronic and optoelectronic devices (Wang et al., 2011b) to energy conversion and storage (Li et al., 2011), such as Li-ion batteries (Liu et al., 2011; Wang et al., 2011a), supercapacitors (Wang Y. J. et al., 2011), and photocatalysis etc. The bicontinuous conductive scaffold used as electrode substrate can provide (1) an interconnected electrolyte-filled pore network that enables rapid mass transport; (2) a large electrode surface area for full exposure of active sites; and (3) high electron conductivity (Liu et al., 2011; Wang Y. J. et al., 2011). These merits give us the chance to address the aforementioned electrocatalyst design limitations in one system. Herein, through a well-designed electrode architecture, we fabricated MnO_2@Ni-pc by using the unique 3D highly ordered conductive scaffold as substrate, which significantly boosted the ORR performance of MnO_2 with high onset potential of 1.04 V and half-wave potential of 0.89 V as well as a large limiting current density of 4.07 mA cm^{-2}, being even comparable to the commercial Pt/C electrocatalyst.

The preparation procedure of the 3D highly ordered bicontinuous porous Ni scaffold (Ni-pc) is schematically illustrated in **Scheme 1** (Please see supporting information for details). Typically, the opal template was prepared by vertical growth of polystyrene spheres (PS, 450 nm, **Figure 1b**) on the surface of conducting glass. Then heating treatment at different temperatures (101, 102, 103, and 104°C. Here 104°C was chosen as the optimum temperature for the following research) for 1 h was carried out to enhance the connection strengths and void spaces between the PS spheres, facilitating Ni electrodeposition (electrodeposition for 1, 2, and 3 h. Here 1 h was chosen as the optimum temperature for following investigation) into the opal template. After removal of PS template, a 3D highly ordered bicontinuous porous Ni scaffold (**Figure 2c** and **Figures S1, S2**) with narrow interconnections between two adjacent spherical voids was formed on the conducting glass. Finally, catalytically active material (MnO_2) for ORR was deposited on the Ni-pc by anodic pulse electrodeposition (electrodeposition for 150, 300, 450 segments were carried out, and 300 segments was choosed for the ORR performance study, denoted as MnO_2@Ni-pc, **Figure 1d** and **Figure S3**).

The thickness of this uniform and 3D bicontinuous Ni-pc was about 10 layers (ca. 2.5 μm) as described in **Figure 2c**. To keep its unique porous structure and obtain both excellent mechanical and electronic contact between the active material and the conductive framework, deposition time of MnO_2 should be carefully controlled (300 segments for 1 h). Relatively short deposition time would give rise to insufficient mass loading of catalyst while prolonged time could cause excessive mass loading, thereby blocking the pores and resulting in poor catalytic performance. As seen from **Figure 2d**, MnO_2 flakes with a moderate thickness evenly grown on the Ni-pc, which gained a high pore volume fraction. This porous structure of MnO_2 @Ni-pc is conducive to sufficient exposure of the active sites of catalysts. Moreover, the nanochannels of Ni-pc remain unblocked during MnO_2 deposition process according to the backside SEM image of MnO_2@Ni-pc (**Figure 1e** and **Figure S4**), which benefits both the O_2 diffusion and electrolyte transmission. Besides, energy dispersive X-ray (EDX) element analysis (**Figure 1f**) for MnO_2@Ni-pc verified the existence of Mn, Ni, and O elements.

The powder X-ray diffraction (PXRD) (**Figure 2a**) pattern was performed to confirm the crystal structure of MnO_2@Ni-pc. The diffraction pattern for MnO_2@Ni-pc has apparent peaks at 37.1, 39.0, and 65.7°, corresponding to (311), (222), and (440) lattice plane of MnO_2 with *Fd*-3*m*(277) space group (JCPDS 44-0992), respectively. The preferred orientation of the electrodeposited manganese oxide on the highly ordered Ni-pc has led to the disappearance of other crystal peaks. In addition, the broadening of peaks indicates the small particle size/thickness of the as-deposited MnO_2. The sharp peak at 44.5° can be indexed to Ni (011) (JCPDS 45-1027), which is attributed to the Ni-pc scaffold.

Surface analysis of MnO_2@Ni-pc was further carried out using X-ray photoelectron spectroscopy (XPS) (**Figures 2b–d**). The XPS survey (**Figure 2b**) indicated the existence of Mn, Ni, O elements. The magnitude of peak splitting is indicative of the Mn oxidation sate (Wu et al., 2012). The high-resolution spectra of Mn 2p and Mn 2s are shown in **Figures 2c,d**, it can be seen that the relative position of Mn $2p_{3/2}$-$2p_{1/2}$ (ΔE 2p) doublet and the multiplet splitting width of Mn 3s (ΔE 3s) are 11.8 and 4.52 eV, respectively, which correspond to Mn(IV) in MnO_2 (Zhang et al., 2011).

To evaluate the enhancement effect of unique 3D highly ordered porous Ni-pc toward catalytic activity of MnO_2, ORR performance of MnO_2@Ni-pc was measured in N_2 or O_2-saturated 0.1 M KOH (**Figure 3**). As seen from **Figure 3a**, CV curves of MnO_2@Ni-pc show no peaks in N_2-saturated electrolyte. However, there exists a well-defined peak potential at about 0.62 V in O_2-saturated electrolyte, which arises from the O_2 reduction reaction (Duan et al., 2013). The linear sweeping voltammograms (LSV) were tested in O_2-saturated 0.1 M KOH with a rotating disk electrode (RDE) at 1600 rpm (**Figure 3b**). For comparison, the bare 3D Ni scaffold (Ni-pc), MnO_2@Ni foil, and 20 wt % Pt/C catalyst were also measured. The LSV curve of MnO_2@Ni-pc shows a half-wave potential ($E_{1/2}$) of 0.89 V, which is even better than Pt/C (0.88 V). The onset potential and limiting current density at 0.2 V of MnO_2@Ni-pc (1.04 V and 4.92 mA cm^{-2}) compared favorably with that of Pt/C (1.05 V and 4.56 mA cm^{-2}). Moreover, MnO_2@Ni-pc exhibits much better catalytic performance than Ni-pc (0.64 V

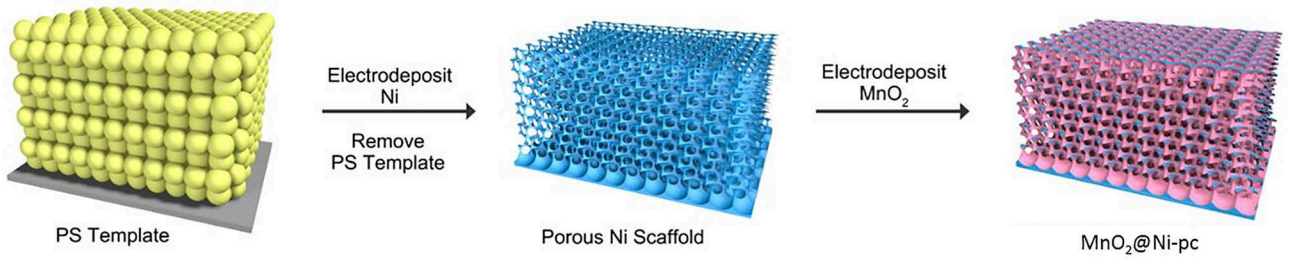

SCHEME 1 | Schematic illustration of the preparation process for MnO_2@Ni-pc.

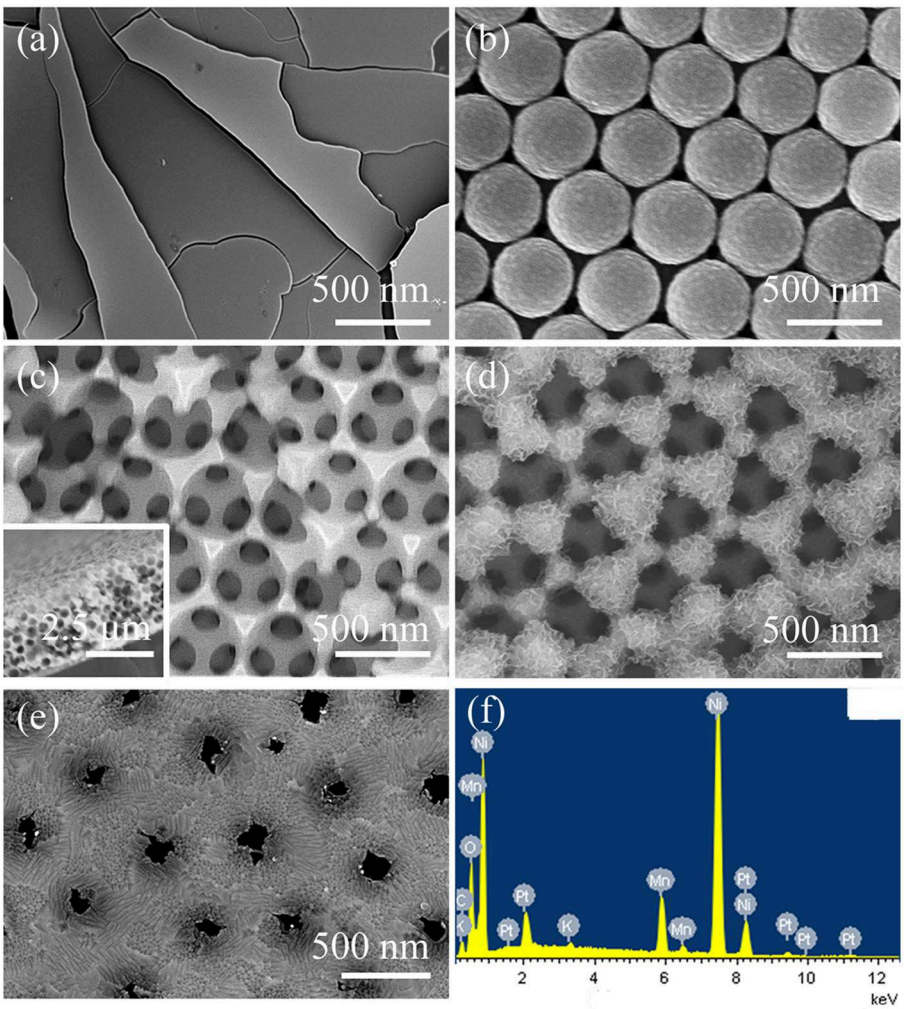

FIGURE 1 | SEM images of **(a)** MnO_2@Ni foil, **(b)** PS opal template on the ITO substrate and **(c)** Ni-pc with the PS opal template annealed at 104°C and Ni electrodeposition for 1 h. Inset is the sectional view of Ni-pc; SEM images of **(d)** the obverse side and **(e)** the back side of MnO_2@Ni-pc (electrodeposition MnO_2 for 300 segments); **(f)** EDX spectrum of MnO_2@Ni-pc.

and 0.89 mA cm^{-2}) and MnO_2@Ni foil (**Figure 2a** 0.71 V and 1.65 mA cm^{-2}).

The number of electrons transferred is an important parameter to evaluating the promotional role of the unique structure of MnO_2@Ni-pc for ORR kinetics. Thus, LSV curves are recorded at different rotating rates (ω) from 400 to 1,600 rpm and corresponding Koutecky-Levich plots (K-L plots) are shown in **Figure 3c** (Zhang and Braun, 2012). The electron

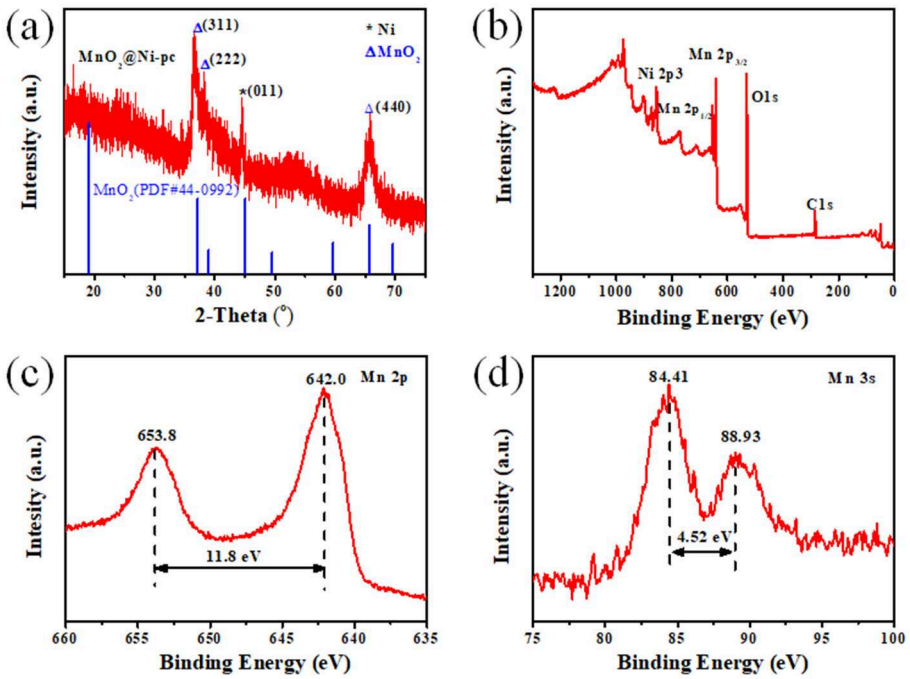

FIGURE 2 | (a) PXRD pattern of MnO_2@Ni-pc; **(b)** XPS survey (0–1,300 eV) of MnO_2@Ni-pc; **(c,d)** High-resolution XPS spectra of **(c)** Mn 2p and **(d)** Mn 3s in MnO_2@Ni-pc.

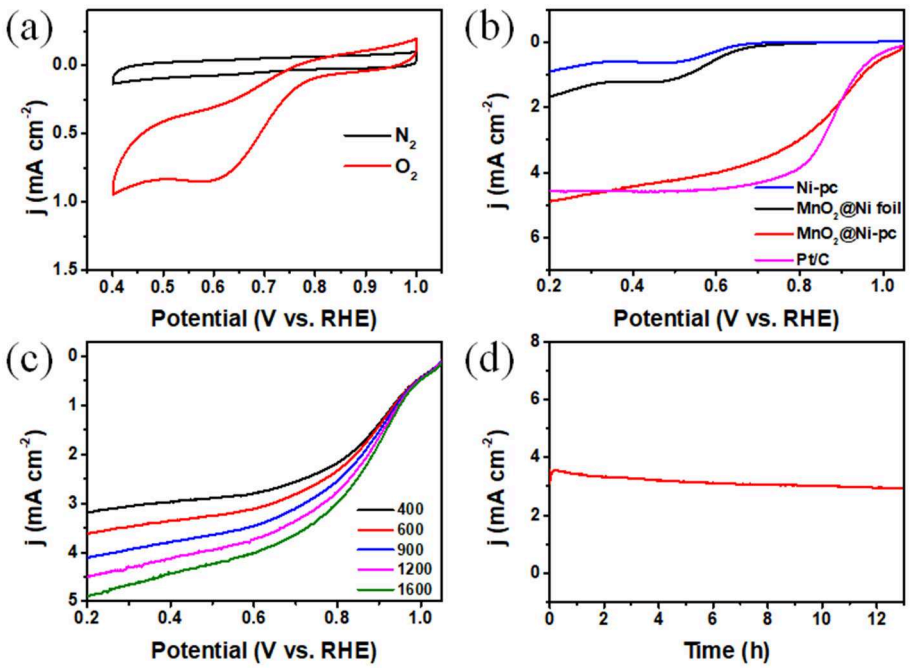

FIGURE 3 | (a) CV curves of MnO_2@Ni-pc in N_2 and O_2-saturated 0.1 M KOH; **(b)** LSV curves of various materials at 1,600 rpm with a sweep rate of 10 mV s^{-1} in O_2-saturated 0.1 M koh; **(c)** LSV curves of MnO_2@Ni-pc at different rotating speeds; **(d)** I-t curve of MnO_2@Ni-pc tested at 0.57 V vs. RHE in O_2-saturated 0.1 M KOH.

transfer number (n) per O_2 of MnO_2@Ni-pc according to the K-L equation (**Figure S5**, see Supporting Information for more details) is ∼3.4 within the potential ranging from 0.2 to 0.5 V, suggesting a great enhancement of ORR kinetics compared to MnO_2 (3.1, 2.7, and 2.3 for pure α-, β-, and γ-MnO_2, respectively) reported before (Wu et al., 2012; Han et al., 2015;

Li et al., 2015, 2019; Lang et al., 2016; Sun et al., 2016; Deng et al., 2017; Wang et al., 2017). Stability of MnO_2@Ni-pc was further tested under a static potential of 0.57 V (**Figure 3d**). The reaction current density for ORR remains stable over 13 h, which exemplify the excellent structural and electrocatalytic stability of MnO_2@Ni-pc. All these experimental results highlight the critical role of the Ni-pc structure for boosting the ORR activity of MnO_2. Ni-pc not only provides bicontinuous conductive scaffold for efficient electron and ion transmission path, but also is in favor of sufficient exposure of active sites and O_2 diffusion (**Figures 2c,d**; Wang et al., 2011a).

In summary, a new MnO_2@Ni-pc nanocomposite with 3D bicontinuous and highly ordered nanoporous structure was fabricated and showed substantially enhanced ORR activity compared with bulk MnO_2@Ni foil (**Figure 1a**), which was even comparable to benchmark Pt/C catalyst. The unique structure of MnO_2@Ni-pc is advantageous for exposing more active sites, accelerating oxygen diffusion, while providing efficient ion and electron pathways during the catalytic process. Rather than being confined to MnO_2 and Ni-pc systems, the presented methodology of attaching active component onto 3D highly ordered conductive skeleton is envisaged to be viable toward improving the performance of other materials such as transition metal dichalcogenides for novel electrochemical applications in supercapacitors, photovoltaic and lithium ion batteries.

DATA AVAILABILITY

All datasets generated or analyzed for this study are included in the manuscript and/or the **Supplementary Files**.

AUTHOR CONTRIBUTIONS

DY conceived the project and designed the experiments. XX and ZF performed the sample preparation, characterization, and electrochemical studies. DY and XX wrote the paper. All authors discussed the results and commented on the manuscript.

ACKNOWLEDGMENTS

We acknowledge the financial support from the National Natural Science Foundation of China (No. 51573214) and Youth Innovation Promotion Association of CAS.

SUPPLEMENTARY MATERIAL

The Supplementary Material for this article can be found online at: https://www.frontiersin.org/articles/10.3389/fmats.2019.00219/full#supplementary-material

REFERENCES

Bashyam, R., and Zelenay, P. (2006). A class of non-precious metal composite catalysts for fuel cells. *Nature* 443:63. doi: 10.1038/nature05118

Chang, C. H., Yuen, T. S., Nagao, Y., and Yugami, H. (2011). Catalytic activity of carbon-supported iridium oxide for oxygen reduction reaction as a Pt-free catalyst in polymer electrolyte fuel cell. *Solid State Ion* 197, 49–51. doi: 10.1016/j.ssi.2011.06.015

Deng, J., Li, H., Wang, S., Ding, D., Chen, M., Liu, C., et al. (2017). Multiscale structural and electronic control of molybdenum disulfide foam for highly efficient hydrogen production. *Nat. Commun.* 8:14430. doi: 10.1038/ncomms14430

Duan, J., Zheng, Y., Chen, S., Tang, Y., Jaroniec, M., and Qiao, S. (2013). Mesoporous hybrid material composed of Mn_3O_4 nanoparticles on nitrogen-doped graphene for highly efficient oxygen reduction reaction. *Chem. Commun.* 49, 7705–7707. doi: 10.1039/C3CC43338B

Gong, M., Li, Y., Wang, H., Liang, Y., Wu, J. Z., Zhou, J., et al. (2013). An advanced Ni-Fe layered double hydroxide electrocatalyst for water oxidation. *J. Am. Chem. Soc.* 135, 8452–8455. doi: 10.1021/ja4027715

Han, X., Chen, F., Chen, C., Hu, Y., and Chen, J. (2015). Uniform MnO_2 nanostructures supported on hierarchically porous carbon as efficient electrocatalysts for rechargeable Li-O_2 batteries. *Nano Res.* 8, 156–164. doi: 10.1007/s12274-014-0604-y

Jaouen, F., Proietti, E., Lefèvre, M., Chenitz, R., Dodelet, J.-P., Wu, G., et al. (2011). Recent advances in non-precious metal catalysis for oxygen-reduction reaction in polymer electrolyte fuel cells. *Energy Environ. Sci.* 4, 114–130. doi: 10.1039/C0EE00011F

Lang, X. Y., Liu, B. T., Shi, X. M., Li, Y. Q., Wen, Z., and Jiang, Q. (2016). Ultrahigh-power pseudocapacitors based on ordered porous heterostructures of electron-correlated oxides. *Adv. Sci.* 3:5. doi: 10.1002/advs.201500319

Lefèvre, M., Proietti, E., Jaouen, F., and Dodelet, J. P. (2009). Iron-based catalysts with improved oxygen reduction activity in polymer electrolyte fuel cells. *Science* 324, 71–74. doi: 10.1126/science.1170051

Li, J., Liu, H., Wang, M., Lin, C., Yang, W., Meng, J., et al. (2019). Boosting oxygen reduction activity with low-temperature derived high-loading atomic cobalt on nitrogen-doped graphene for efficient Zn-air batteries. *Chem. Commun.* 55, 334–337. doi: 10.1039/C8CC08992B

Li, J., Wang, Y., Zhou, T., Zhang, H., Sun, X., Tang, J., et al. (2015). Nanoparticle superlattices as efficient bifunctional electrocatalysts for water splitting. *J. Am. Chem. Soc.* 137, 14305–14331. doi: 10.1021/jacs.5b07756

Li, Y., Zhao, Y., Cheng, H., Hu, Y., Shi, G., Dai, L., et al. (2011). Nitrogen-doped graphene quantum dots with oxygen-rich functional groups. *J. Am. Chem. Soc.* 134, 15–18. doi: 10.1021/ja206030c

Liu, R., Wu, D., Feng, X., and Müllen, K. (2011). Bottom-up fabrication of photoluminescent graphene quantum dots with uniform morphology. *J. Am. Chem. Soc.* 133, 15221–15223. doi: 10.1021/ja204953k

Morozan, A., Campidelli, S., Filoramo, A., Jousselme, B., and Palacin, S. (2011a). Catalytic activity of cobalt and iron phthalocyanines or porphyrins supported on different carbon nanotubes towards oxygen reduction reaction. *Carbon* 49, 4839–4847. doi: 10.1016/j.carbon.2011.07.004

Morozan, A., Jousselme, B., and Palacin, S. (2011b). Low-platinum and platinum-free catalysts for the oxygen reduction reaction at fuel cell cathodes. *Energy Environ. Sci.* 4, 1238–1254. doi: 10.1039/c0ee00601g

Sun, L., Yang, M., Huang, J., Yu, D., Hong, W., and Chen, X. (2016). Freestanding graphitic carbon nitride photonic crystals for enhanced photocatalysis. *Adv. Funct. Mater.* 26, 4943–4950. doi: 10.1002/adfm.201600894

Wang, M., Lin, M., Li, J., Huang, L., Zhuang, Z., Lin, C., et al. (2017). Metal-organic framework derived carbon-confined Ni_2P nanocrystals supported on graphene for an efficient oxygen evolution reaction. *Chem. Commun.* 53:8372. doi: 10.1039/C7CC03558F

Wang, S., Iyyamperumal, E., Roy, A., Xue, Y., Yu, D., and Dai, L. (2011a). Vertically aligned BCN nanotubes as efficient metal-free electrocatalysts for the oxygen reduction reaction: a synergetic effect by co-doping with boron and nitrogen. *Angew. Chem. Int. Ed.* 50, 11756–11760. doi: 10.1002/anie.201105204

Wang, S., Yu, D., Dai, L., Chang, D. W., and Baek, J. B. (2011b). Polyelectrolyte-functionalized graphene as metal-free electrocatalysts for oxygen reduction. *ACS Nano* 5, 6202–6209. doi: 10.1021/nn200879h

Wang, Y. J., Wilkinson, D. P., and Zhang, J. (2011). Noncarbon support materials for polymer electrolyte membrane fuel cell electrocatalysts. *Chem. Rev*. 111, 7625–7651. doi: 10.1021/cr100060r

Wu, G., More, K. L., Johnston, C. M., and Zelenay, P. (2011). High-performance electrocatalysts for oxygen reduction derived from polyaniline, iron, and cobalt. *Science* 332, 443–447. doi: 10.1126/science.1200832

Wu, Z. S., Yang, S., Sun, Y., Parvez, K., Feng, X., and Müllen, K. (2012). 3D nitrogen-doped graphene aerogel-supported Fe_3O_4 nanoparticles as efficient electrocatalysts for the oxygen reduction reaction. *J. Am. Chem. Soc*. 134, 9082–9085. doi: 10.1021/ja3030565

Zhang, H., and Braun, P. V. (2012). Three-dimensional metal scaffold supported bicontinuous silicon battery anodes. *Nano Lett*. 12, 2778–2783. doi: 10.1021/nl204551m

Zhang, H., Yu, X., and Braun, P. V. (2011). Three-dimensional bicontinuous ultrafast-charge and-discharge bulk battery electrodes. *Nat. Nanotechnol*. 6:277. doi: 10.1038/nnano.2011.38

Zhou, W., Ge, L., Chen, Z. G., Liang, F., Motuzas, J., Xu, H., et al. (2011). Amorphous iron oxide decorated 3D heterostructured electrode for highly efficient oxygen reduction. *Chem. Mater*. 23, 4193–4198. doi: 10.1021/cm201439d

Conflict of Interest Statement: The authors declare that the research was conducted in the absence of any commercial or financial relationships that could be construed as a potential conflict of interest.